energies

MDPI

Article

The Effect of Air Parameters on the Evaporation Loss in a Natural Draft Counter-Flow Wet Cooling Tower

Wei Yuan, Fengzhong Sun *, Ruqing Liu, Xuehong Chen and Ying Li

School of Energy and Power Engineering, Shandong University, Jinan 250061, China; 201620340@mail.sdu.edu.cn (W.Y.); liuruqingsdu@163.com (R.L.); 201612852@mail.sdu.edu.cn (X.C.); 201920472@mail.sdu.edu.cn (Y.L.)

* Correspondence: sfzh@sdu.edu.cn; Tel.: +86-0531-88395691

Received: 22 October 2020; Accepted: 23 November 2020; Published: 24 November 2020

Abstract: The measures to reduce the impact of evaporation loss in a natural draft counter-flow wet cooling tower (NDWCT) have important implications for water conservation and emissions reduction. A mathematical model of evaporation loss in the NDWCT was established by using a modified Merkel method. The NDWCTs in the 300 MW and 600 MW power plant were taken as the research objects. Comparing experimental values with calculated values, the relative error was less than 3%. Then, the effect of air parameters on evaporation loss of NDWCT was analyzed. The results showed that, with the increase of dry bulb temperature, the evaporation heat dissipation and the evaporation loss decreased, while the rate of evaporation loss caused by unit temperature difference increased. The ambient temperature increased by 1 °C and the evaporation loss was reduced by nearly 26.65 t/h. When the relative air humidity increased, the evaporation heat dissipation and evaporation loss decreased, and the rate of evaporation loss caused by unit temperature difference decreased. When relative air humidity increased by 1%, the outlet water temperature rose by about 0.08 °C, and the evaporation loss decreased by about 5.63 t/h.

Keywords: natural transfer; mathematical modeling; Merkel approach; evaporation loss; dry bulb temperature; relative air humidity

1. Introduction

NDWCTs are extensively used in most electric power industries to reject waste heat in the condenser to the surrounding. The cooling process in NDWCT, as an extremely important process in power production, is realized by contact heat dissipation and evaporation heat dissipation. The water loss of the NDWCT mainly includes evaporation loss, drift loss and blowdown loss. Evaporation loss is the largest water consumption project in power plants. Moreover, the "white smoke" from the NDWCT outlet will pollute the surrounding environment. Therefore, reducing the impact of evaporation loss in NDWCT has important implications for water conservation and emissions reduction.

Water, as a heat transfer medium in NDWCTs, is the scarce resources in many areas [1–3]. Among many cooling methods, direct air-cooled system has significant advantage of water saving. Several elements, such as the ambient wind speed, wind direction, fan performance, and the installation angles of its blades, affect the thermal-flow characteristics of an air-cooled system tremendously [4–8]. However, compared with wet cooling towers, dry cooling towers only account for a very small proportion.

Evaporation loss is an important part of water consumption in power plants. Based on the heat and mass transfer equations, Kairouani et al. [9] presented a mathematical model for prediction of the evaporation loss for cooling towers, and obtained an optimal water loss which was equivalent to 4% of the total water flow rate. Xia et al. [10] used the Merkel method, the Poppe approach

and empirical equation to numerically calculate the evaporation loss for NDWCT. Their results showed that neither the Merkel method nor the empirical equation can predict the evaporation loss as accurately as the Poppe approach. Facao and Oliveira [11] established a computational fluid dynamics (CFD) model to analyse the mass and heat transfer in the cooling tower. Qureshi and Zubair [12,13] proposed an empirical relation for studying the evaporation losses in wet cooling towers based on the ASHRAE's rule of thumb, and the results showed that the percentage of water evaporation obtained from the empirical relation agreed well with experimental data. Hajidavalloo et al. [14] developed a conventional mathematical model to study the effect of wet bulb temperature on the thermal performance of cross flow cooling towers, and found that the approach, range and evaporation loss gradually increased with the increase of wet bulb temperature. Moreover, the variation between ratio of evaporation loss to circulating water and Variation was obtained. Based on the Poppe approach and mixed-integer nonlinear programming, Rubio-Castro et al. [15] presented an optimal design algorithm for a mechanical ventilation cooling tower. Similarly, for optimal designing the mechanical draft cooling tower, Rao and More [16] developed a self-adaptive Jaya algorithm. The optimal total cost of tower geometry obtained by the Merkel method, Poppe approach, artificial bee colony algorithm, and this self-adaptive Jaya algorithm were compared with each other. The result showed that the optimal total cost of tower geometry obtained by the method of the self-adaptive Jaya algorithm was the least. Naik et al. [17] obtained the thermal performances of mechanical ventilation cooling tower by developing a simple analytical model and discovered that the operating parameters had important effect on heat and mass transfer of cooling tower. Based on the effectiveness- number of transfer unit (e-NTU) method, Mansour and Hassab [18] developed a new correlation which was adopted to study the thermal performance of wet counterflow cooling tower. Picardo and Variyar [19] established a new methodology for studying the packed height in a cooling tower, and found that packed height of the cooling tower had nothing to do with mass flow rate of circulating water and tower diameter, but was related to excess air flow. Fisenko et al. [20] developed a new mathematical model of a mechanical draft cooling tower performance, the precision of which is about 3%. It was found that the average cube of the droplet radius practically determines thermal efficiency. Chen et al. [21] adopted a transient one-dimensional mathematical model to study the adsorption chiller. The results showed that the cooling power and coefficient of performance (COP) could be calculated by the model given the following conditions, including the hot water inlet temperature, the chilled water inlet temperature, the air inlet wet bulb temperature, and dry bulb temperature.

So far, the mathematical model of evaporation loss mainly lays a lot of emphasis on mechanical wet cooling towers. Seldom key studies focus on the effect of air parameters on evaporation loss in NDWCTs. In this study, the NDWCTs in the representative 300 MW and 600 MW power plant were taken as the subject investigated. Based on the Merkel method, a mathematical model of evaporation loss in the NDWCT was established in view of evaporation loss. Then a solution program for this model was developed by MATLAB software. The accuracy of the mathematical model was verified by comparing experimental values with calculated values. The NDWCTs were needed for operating in a variation of air parameters which strongly affected the thermal performance of NDWCTs. The influence mechanism of air parameters on evaporation loss in the NDWCT was mainly analyzed, which was of great guiding significance for the power plant to reduce the emission and save water.

2. Mathematical Model

The heat transfer of circulating water was achieved by contact heat dissipation and evaporation heat dissipation in NDWCTs. The circulating water after heat transfer in condensers was pressurized by circulating water pump, and the circulating water passed through spray zone, fill zone, rain zone and then fell into collecting basin in turn. While, ambient air flowed upward. For an existing NDWCT, the thickness of the tower is about 1 m, and the tower tube of NDWCT is a cast-in-place reinforced concrete thin shell structure. The inner wall of the tower tube is brushed with anticorrosive paint, the outer wall of the tower tube is brushed with cement slurry, and the inner wall of the collecting

basin is brushed with waterproof mortar. In this study, the important assumptions of the model were as follow:

- The conditions of water and air varied only with vertical position in the tower.
- Radiation heat transfer from air to water was negligible.
- Heat transfer through the tower wall to the environment was negligible.
- Temperatures of water and air at any cross-sections were uniform.
- Windage and blowdown losses were negligible.

Based on Merkel theory, the enthalpy difference was taken as the sole driving force for the heat dissipation. In this theory, the assumptions that the change of circulating water was negligible and the Lewis factor was equal to 1 were adopted [10,18].

The Merkel equation as follows:

$$\frac{h_d A_t}{m_w} = \int_{T_{wo}}^{T_{wi}} \frac{c_{pw} dT_w}{i_{masw} - i_{ma}} \tag{1}$$

where h_d is mass transfer coefficient. i_{masw} is the enthalpy of the saturated air layer on the water surface when water temperature is T_w. i_{ma} is the enthalpy of the moist air when air temperature is T_a.

The Merkel number was modified in view of the effects of water loss. In this study, introduction of a heat coefficient k that represented the heat carried by evaporation loss [22,23]. The validity range of k was that the circulating water temperature range was in the range of 0–50 °C. Then, the modified Merkel equation is as follows:

$$Me_M = \frac{1}{k} \int_{T_{wo}}^{T_{wi}} \frac{c_{pw} dT_w}{i_{masw} - i_{ma}} \tag{2}$$

where T_{wi}, and T_{wo} are the inlet water temperature and outlet water temperature of NDWCT respectively.

The specific derivative process of k coefficient was detailed introduced here [23], Figure 1 shows the heat and mass transfer in a finite volume of the cooling tower. As shown in Figure 1, the heat dissipating capacity of water was equal to the heat absorption capacity of air, as described in Equation (3).

$$c_{pw} d(m_w T_w) = h_d (i_{masw} - i_{ma}) A_V dz \tag{3}$$

where c_{pw} = 4.1868 kJ/(kg·°C) is the specific heat of water, m_w is the circulating water flow rate, T_w is the circulating water temperature, i_{ma} is the air enthalpy, and i_{masw} is the enthalpy of saturated vapor with the temperature of T_w.

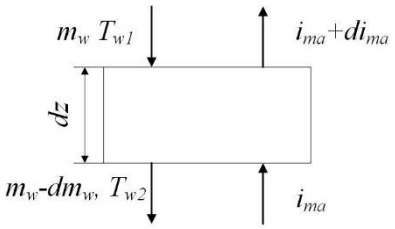

Figure 1. Heat and mass transfer in a finite volume of the cooling tower.

Here, introducing k, Equation (3) could be reduced to Equation (4) as follows:

$$c_{pw} d(m_w T_w) = \frac{1}{k} c_{pw} m_w dT_w = h_d (i_{masw} - i_{ma}) A_V dz \tag{4}$$

For a finite volume with an inlet water temperature T_{w1} and an outlet water temperature of T_{w2}, the heat dissipating capacity of water could be calculated as Equation (5).

$$c_{pw}[m_w T_{w1} - (m_w - \Delta m_w)T_{w2}] = \frac{1}{k} c_{pw} m_w dT_w \tag{5}$$

According to Equation (5), the computational formula for k was:

$$k = \frac{1}{1 + \frac{T_{w2}\Delta m_w}{m_w \Delta T_w}} \tag{6}$$

The heat dissipating capacity included conduction heat dissipation Q_c and evaporation heat dissipation Q_e, that was,

$$c_{pw} m_w dT_w = Q_c + Q_e \tag{7}$$

According to Equations (6) and (7), the k was calculated by:

$$k = \frac{1}{1 + \frac{c_{pw} T_{w2}}{\gamma_{T_{w2}} \varepsilon}}, \ \varepsilon = \frac{Q_e}{Q_c + Q_e} \tag{8}$$

where $\gamma_{T_{w2}}$ is the latent heat of vaporization at the temperature of T_{w2}. When T_{w2} is in the range of 0–50 °C, the $\gamma_{T_{w2}}$ could be calculated as follows:

$$\gamma_{T_{w_2}} = 2453.46 - 2.3446(T_{w2} - 20) \tag{9}$$

Because the Q_e is much larger than Q_c in summer and $T_{w2} c_{pw} << \gamma_{T_{w2}}$, the Equation (8) can be simplified as follows:

$$k \approx \frac{1}{1 + \frac{c_{pw} T_{w2}}{\gamma_{T_{w2}}}} \approx 1 - \frac{c_{pw} T_{w2}}{\gamma_{T_{w2}}} + \left(- \frac{c_{pw} T_{w2}}{\gamma_{T_{w2}}} \right)^2 + \ldots \approx 1 - \frac{c_{pw} T_{w2}}{\gamma_{T_{w2}}} \tag{10}$$

According to Equations (9) and (10), the k was calculated by:

$$k = 1 - \frac{T_{w2}}{586 - 0.56(T_{w2} - 20)} \tag{11}$$

For whole cooling tower k was expressed as

$$k = 1 - \frac{T_{wo}}{586 - 0.56(T_{wo} - 20)} \tag{12}$$

The pumping force H and resistance of the NDWCT Z were equal. Ambient air entered the NDWCT from the inlet of tower, passed through the rain zone, fill zone, spray zone, water collector, and drained from the tower exit, generating resistance as the air passes through these parts. On the other hand, the pumping force was H caused by the density difference inside and outside the NDWCT [23].

$$H = (\rho_{ai} - \rho_{ao}) g (H_t - H_{inlet}), Z = \frac{1}{2} \xi \rho_{am} v_{am}^2, \ H = Z \tag{13}$$

where H is the pumping force, Z is the resistance of cooling tower, ρ_{ai} is tower inlet air density, ρ_{ao} is tower outlet air density, H_t is the tower height, and H_{inlet} is the tower inlet height. ξ is total drag coefficient of the tower and v_{am} is the average airflow velocity in packing section.

Evaporation loss equaled the increase of air moisture content in NDWCT. The formula for calculating the evaporation loss was as follows:

$$m_{evap} = m_a (w_o - w_i) \tag{14}$$

The calculation formula of conduction heat dissipation was:

$$Q_c = c_{pa} m_a (T_{ao} - T_{ai}) \tag{15}$$

where Q_c is the conduction heat dissipation of cooling tower, c_{pa} is the specific heat of air, and T_{ai} and T_{ao} are the inlet temperature and the outlet temperature of the cooling tower.

The mass flow of air was:

$$m_a = \rho_{ai} v_{am} A_s \tag{16}$$

where A_s is the area of cross section of fill and ρ_{ai} is tower inlet air density.

Here, the calculation method of the outlet air temperature T_{ao} was introduced in detail. It can be seen from the enthalpy and humidity diagram that when the dry bulb temperature was greater than 15 °C, the saturation enthalpy of air and the dry bulb temperature were basically linear. It was generally considered that the humid air at the outlet of the cooling tower was saturated or close to saturation, thus here i_{ao} was used instead of i''_{ao}

$$\frac{T_{ao} - T_{ai}}{T_{wm} - T_{ai}} = \frac{i''_{ao} - i''_{ai}}{i''_m - i''_{ai}} \approx \frac{i_{ao} - i''_{ai}}{i''_m - i''_{ai}} \Rightarrow T_{ao} = T_{ai} + (T_{wm} - T_{ai}) \frac{i_{ao} - i''_{ai}}{i''_m - i''_{ai}} \tag{17}$$

where T_{ai} and T_{ao} are the inlet temperature and the outlet temperature of the cooling tower, i''_{ai} and i''_{ao} are the specific enthalpy of saturated air at temperature T_{ai} and T_{ao} respectively, i_{ao} is the enthalpy of the outlet air of the cooling tower, T_{wm} is the average temperature of temperature T_{wi} and T_{wo}, i''_m is the specific enthalpy of saturated air at temperature T_{wm}.

As shown in Figure 1, the heat dissipating capacity of water was equal to the heat absorption capacity of air. The heat absorption capacity of air was equal to the increase of air enthalpy, as shown in Equation (18).

$$\frac{1}{k} c_{pw} m_w dT_w = m_a di_{ma}, \text{ after integration, } i_{ao} = i_{ai} + \frac{c_{\mathrm{pw}} (T_{wi} - T_{wo}) m_w}{m_a k} \tag{18}$$

The physical modelling experiment of the fillers in NDWCT is carried out, and then the fitting formula of Merkel number and gas-water ratio was obtained.

$$Me'_M = C\lambda^n \tag{19}$$

where λ is the ratio of the mass air flow rate to the mass flow rate of circulating water. C and n are constants obtained from thermal performance test of the packing in the simulation test tower. The values of C and n were shown in Table 1.

Table 1. The values of C and n.

Capacity	300 MW	600 MW
C	1.69	2.19
n	0.54	0.65

The geometric dimension parameters, such as air inlet height of tower, the tower height, drenching area, average diameter of tower inlet, and tower outlet diameter, for the existing NDWCT, were determined. The environmental parameters, including atmospheric pressure, dry bulb temperature, wet bulb temperature and relative humidity, were given. Through MATLAB programming iterative calculation to obtain the outlet water temperature of the NDWCT, the tower air volume and the tower air moisture content. Finally, the evaporation loss in the NDWCT was obtained. The program block diagram for solving this calculation model is shown in Figure 2.

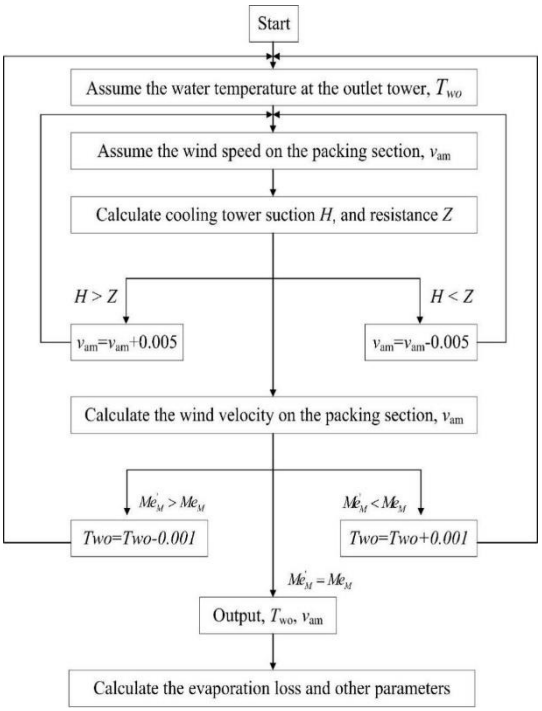

Figure 2. The flowchart of the evaporation loss in NDWCT.

3. Experimental Verification

In this study, taking the NDWCTs of the representative 300 MW and 600 MW power plant as the experimental objects. The geometric dimensions and filler characteristics are shown in Table 2. The experiment was conducted in the northern of China, and the whole experiment was conducted in summer. Figure 3 shows the schematic diagram of NDWCT and the location of monitoring points. The NDWCT included the collecting basin, fillers, water distribution system, tower shell and the cooling tower central shaft. After being pressurized by the water pump, the hot water enters the water distribution system through the shaft, and then falls into the collecting zone after passing through the fill zone, as shown by the red arrow in the Figure 3. At the same time, under the cooling tower pumping force, the air passed through the rain zone, the fill zone, and the spray zone in turn and was finally discharged out of the tower, as shown by the black arrow in the Figure 3.

Table 2. Geometric dimensions of the NDWCT.

	Capacity	**300 MW**	**600 MW**
Geometric dimensions	Tower height (m)	123.4	150.6
	Air inlets' height (m)	8.3	9.8
	Distance between spray zone and tower outlet (m)	113.5	137.6
	Air inlet diameter (m)	84.7	115.7
	Outlet diameter (m)	52.5	72.0
	Area of fill zone (m^2)	5500	9000
Filler characteristics	Fitting formula of fillers	$Me'_M = 1.69\lambda^{0.54}$	$Me'_M = 2.19\lambda^{0.65}$

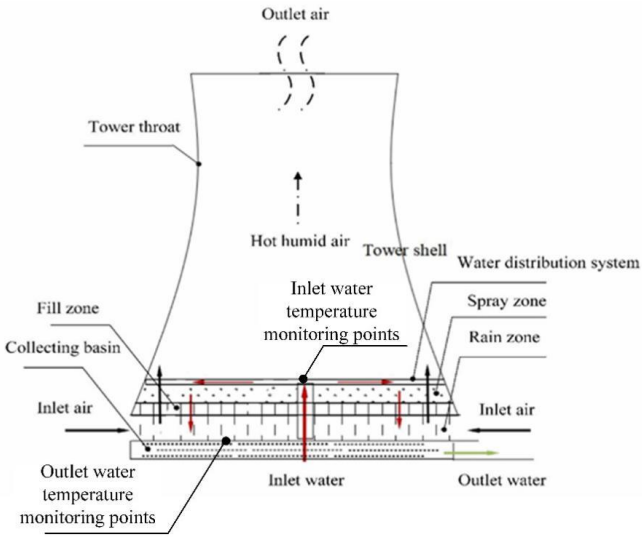

Figure 3. Schematic diagram of NDWCT and the location of monitoring points.

Two layers of temperature measuring points were arranged in the NDWCT, which mainly measured the water temperature at the inlet and outlet of the cooling tower. The monitoring points of inlet and outlet tower water temperature were respectively location in the central shaft and surface of collecting basin, as shown in Figure 3. The equal area method was used to measure the outlet tower water temperature. The location distribution of collecting basin measuring point were shown in in Figure 4, and the radius of the measuring point was obtained by Equation (20). Meteorological parameters around the NDWCT were measured by a small meteorological station. In order to improve the accuracy of measurements, the small-type meteorological station was located 40 m away from the NDWCT and 3 m above the horizontal level. The testing instruments at various cooling zones were listed in Table 3.

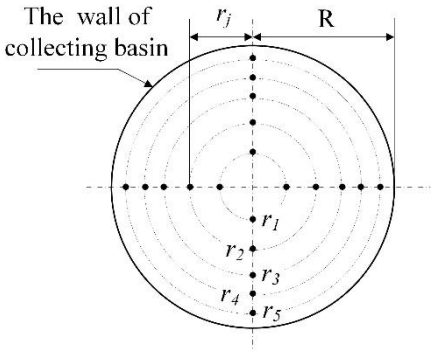

Figure 4. Sectional view of collecting basin mearing point.

Table 3. Testing instruments.

Item	Testing Instrument	Accuracy
Atmospheric pressure	Small-type meterological station	±1.5%
Inlet dry and wet bulb temperature	Small-type meterological station	±0.1 °C
Inlet and outlet tower water temperature	Platinum resistance thermometer	±0.1 °C
Mass flow rate of circulating water	FLEXIM ultrasonic flowmeter	±0.5%

In this study, the experimental data were transmitted instantly through wireless technology, and the experimental data acquisition system was shown in the Figure 5. Taking temperature measurement as an example, the temperature at the measuring point was transformed into current

signal through the sensor, and the current signals was received and sent to the signal receiving device by the data acquisition device. Next, the current signal was analyzed by software to get the corresponding temperature value in computer.

$$r_j = R\sqrt{(2j-1)/10} \tag{20}$$

where j is the coordinates of the laps where the measuring point is located, and the value of j is 1, 2, 3, 4, and 5 from the center along the radial direction. r_j is the radius of the measuring point in the lap j. R is the radius of collecting basin.

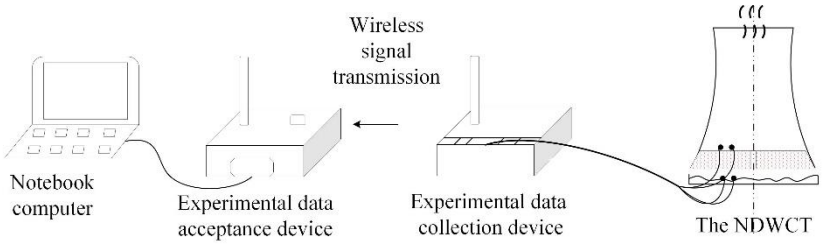

Figure 5. Schematic diagram of experimental data acquisition.

In this paper, the accuracy of the mathematical model was verified by experimental data. The temperature in the center of the shaft was set as the inlet water temperature of the NDWCT. The average temperature of the temperature measuring point of the collecting basin was used as the outlet water temperature of NDWCT. Five different operating conditions of the 300 MW and 600 MW NDWCTs were tested respectively. More specifically, atmospheric pressure, dry bulb temperature, wet bulb temperature, mass flow rate of circulating water, and inlet tower water temperature are shown in Tables 4 and 5.

Table 4. Five different working conditions of 300 MW NDWCT.

Working Conditions	Meteorological Parameters			Mass Flow Rate of Circulating Water (t/h)	Inlet Tower Water Temperature (°C)
	Atmospheric Pressure (kPa)	Dry Bulb Temperature (°C)	Wet Bulb Temperature (°C)		
1	99.6	26.5	19.9	38286	38.2
2	100.1	31.1	26.4	38286	41.4
3	100.8	26.7	21.0	22746	41.7
4	100.1	30.9	26.6	38286	41.1
5	100.4	28.6	23.6	38286	38.8

Table 5. Five different working conditions of 600 MW NDWCT.

Working Condition	Meteorological Parameters			Mass Flow Rate of Circulating Water (t/h)	Inlet Tower Water Temperature (°C)
	Atmospheric Pressure (kPa)	Dry Bulb Temperature (°C)	Wet Bulb Temperature (°C)		
1	100.4	31.98	27.90	74272	41.34
2	101.1	27.52	25.40	74272	38.06
3	101.1	28.16	25.40	74272	38.49
4	101.1	27.59	24.21	74272	37.02
5	101.1	28.32	23.67	74272	38.36

The verification of this mathematical model was made by comparing the outlet water temperature T_{wo} obtained from the mathematical model with the experimental value. Figure 6 showed the calculated

and experimental values of outlet water temperature T_{wo} at different conditions. By analyzing the calculated and experimental values T_{wo} of 300 MW and 600 MW units respectively, it is found that the calculated value of the outlet water temperature is very close to the experimental value. The maximum relative errors between the calculated and experimental values T_{wo} of the 300 MW and 600 MW unit at five working conditions were 0.95% and 1.20%, respectively. Therefore, it can be considered that the established mathematical model for predicting evaporation loss was accurate, and it was feasible to use this model for the next research.

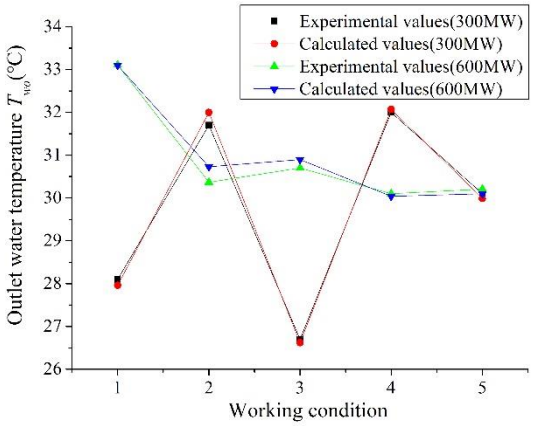

Figure 6. Calculated and experimental values of outlet water temperature at five working conditions.

4. Results and Discussion

The structural parameters of the NDWCT had been determined. Therefore, the influence of geometric dimension parameters wasn't considered. Factors, which affected thermal performance of the NDWCT, would affect evaporation heat dissipation. In this study, the influence of air parameters on evaporation loss was emphatically analyzed. Air parameters mainly included air-dry bulb temperature and relative air humidity. In this paper, The NDWCT 300 MW was selected as the study subject, and the working condition 4 was selected as the reference working conditions. At this time, the relative humidity of the air is 71.79% and specific operating parameters were shown in Table 4.

4.1. Relative Air Humidity

Compared to the reference working condition, only the relative air humidity changed. Figure 7 showed the relationship between outlet water temperature and relative air humidity, which showed that with the increase of the relative air humidity, the outlet water temperature increased. When relative air humidity increased by 1%, the outlet water temperature rose by about 0.08 °C. The main reason was that the driving force of evaporation heat dissipation was the difference between the moisture content of the saturated air layer on the surface of the circulating water and the air moisture content. Hence, when the relative air humidity became larger, the mass transfer decreased. The driving force for the contact heat dissipation was the temperature difference between air and circulating water. Although the relative air humidity increased, the air-dry bulb temperature unchanged. At this time, the contact heat dissipation in the cooling tower remained unchanged. The evaporation heat dissipation in the cooling tower was weakened and the contact heat dissipation remains unchanged, so outlet water temperature of the tower would increase. Later, when the outlet water temperature increased, the temperature between the circulating water temperature and the air temperature became larger, and the contact heat dissipation increased. The increase in contact heat transfer was less than the decrease in evaporation heat transfer.

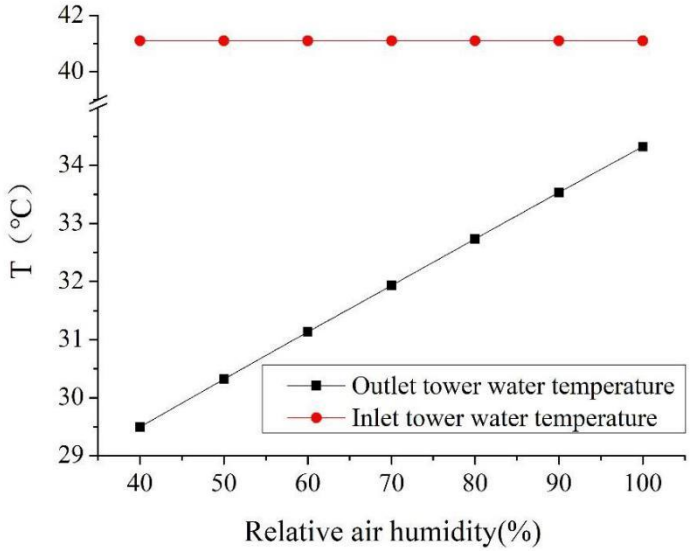

Figure 7. Outlet tower water temperature and relative air humidity.

Figure 8 showed the relationship between evaporation loss and relative air humidity. Notably, with the increase of the relative air humidity, the evaporation loss decreased significantly. When relative air humidity increased by 1%, the evaporation loss decrease by about 5.63 t/h. The trend of evaporation loss with environmental humidity was also compared with Xia's [10] research results. Xia used the Merkel method, the Poppe approach and empirical equation to numerically analyse the effect the relative air humidity on the evaporation loss for NDWCT, as shown in Figure 9. Since the structural parameters, environmental parameters and operating parameters of the selected cooling tower were not the same as those of Xia, here only qualitative analysis and comparison were made on Figures 8 and 9. When the methods of Merkel method and empirical equation were used, the evaporation loss decreased with the relative air humidity increasing. When the Poppe approach was used, the evaporation loss remained stable as the relative air humidity increased. Poppe approach believed that the air could reach supersaturation, which meant that when the air had reached saturation, it could still continue to contain water. However, the outlet air of the cooling tower can generally only reach saturation or near saturation. Therefore, Poppe approach was not suitable for analysis of evaporation loss with different humidity. According to Xia's conclusion, the evaporation loss was more than the actual value by using empirical equation, while the evaporation loss was lower than the actual value by using Merkel method. In this study, the trend of evaporation loss with different humidity was similar to that when Xia used Merkel method and empirical equation. However, in this study, taking into account the influence of evaporation loss, Merkel method was modified so that the evaporation loss agreed with the test value, which was explained in the model verification. Both qualitative and quantitative analysis could be done on the research of cooling tower evaporation loss by using this modified Merkel method.

With the increase of relative air humidity, the evaporation heat dissipation driven by the difference in moisture content of air decreased. The air-dry bulb temperature did not change with the increase of relative air humidity. The driving force of contact heat dissipation almost unchanged. At this time, with relative air humidity increasing, contact heat dissipation basically unchanged. Later, when the outlet water temperature increased, the contact heat dissipation increased, and the total heat dissipation decreased. Thus, the proportion of the contact heat dissipation to the total heat dissipation increased, as shown in Figure 10. To comprehensively evaluate evaporation loss in the NDWCT, the relative variation of evaporation loss should also be considered. In this study, a parameter K_e, the physical significance of which was the ratio of evaporation loss to total circulating water at per 1 °C temperature drop, was defined as an index to evaluate the relative variation of evaporation loss. K_e decreased with the increase of relative air humidity, as shown in Figure 11.

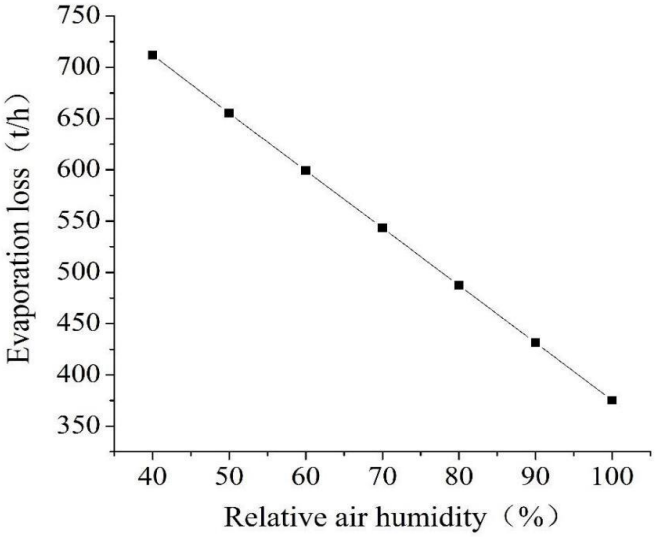

Figure 8. Evaporation loss at vary relative air humidity.

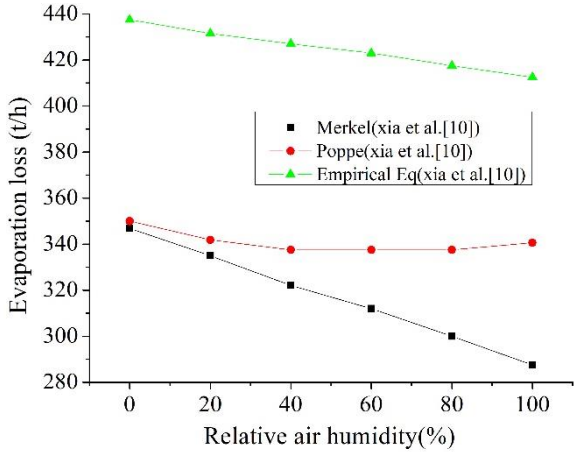

Figure 9. Variation in evaporation loss calculated by Xia [10].

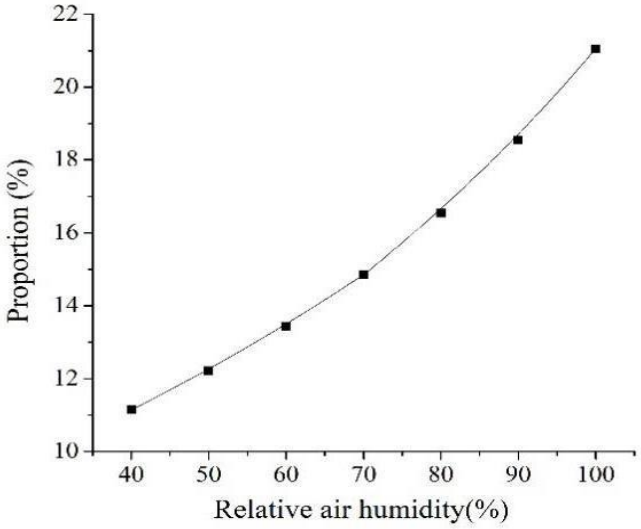

Figure 10. Relationship between the proportion of contact heat dissipation to total heat dissipation and relative air humidity.

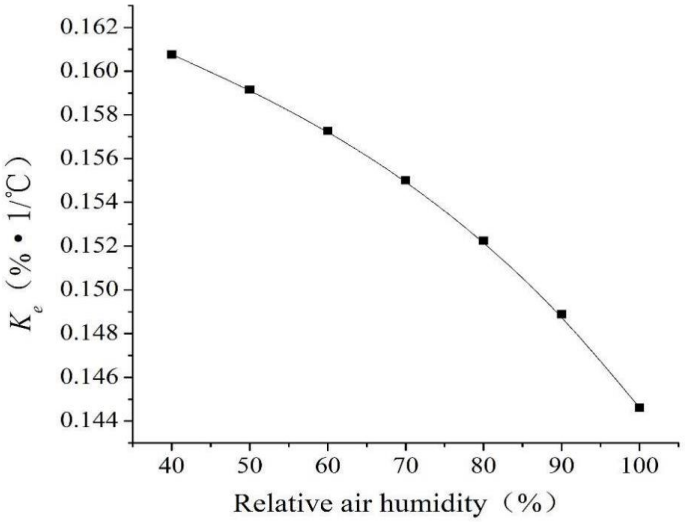

Figure 11. Relationship between K_e and relative air humidity.

4.2. Air-Dry Bulb Temperature

Compared with the reference working condition, only the air-dry bulb temperature changed and other parameters remained unchanged. When the low-temperature air passed through high-temperature circulating water, heat was transferred from the higher temperature side to the lower temperature side. The driving force for heat transfer was the temperature difference between air and circulating water. When the air-dry bulb temperature increased, the temperature difference between the air and the circulating water decreased, and the heat transfer decreased. The surface of the circulating water formed a thin layer of saturated air whose temperature was the same as that of the circulating water. The speed of mass transfer depended on the difference between the moisture content in the saturated air layer and the moisture content in the air. When the air temperature increased, the moisture content in the air also increased, which caused the difference between the saturated air layer on the surface of the circulating water and the moisture content in the air to decrease, so the mass transfer also decreased. Hence, with the increase of air-dry bulb temperature, the heat and mass transfer performance of the NDWCT deteriorated, which led to a gradual increase in the outlet water temperature, as shown in Figure 12. When the air-dry bulb temperature gradually increased, the evaporation loss decreased significantly, as shown in Figure 13. When air dry bulb temperature increased by 1 °C, the outlet tower water temperature increased by about 0.59 °C and the evaporation loss dropped by nearly 26.65 t/h.

With the increase air-dry bulb temperature, the temperature difference between circulating water and air decreased gradually. Thus, the driving force of contact heat dissipation decreased, and contact heat dissipation in the NDWCT decreased. In addition, with the air-dry bulb temperature increasing, the relative air humidity remained unchanged and the moisture content of inlet tower air increased, which weaken the driving impetus of evaporative heat dissipation. With air-dry bulb temperature increasing, the contact heat dissipation and evaporation heat dissipation capacity of the NDWCT were both weakened. However, the increase of air-dry bulb temperature had a greater impact on the contact heat dissipation capacity driven by temperature difference. Figure 14 showed that the proportion of contact heat dissipation to total heat dissipation was decreased with the increase of air-dry bulb temperature. Figure 15 showed the relationship between K_e and air-dry bulb temperature. The temperature drop of circulating water in the NDWCT was mainly achieved by the evaporation heat dissipation. When the inlet tower water temperature, the mass flow rate, and the relative humidity were kept unchanged, K_e increased with the rise of air-dry bulb temperature as shown in Figure 15.

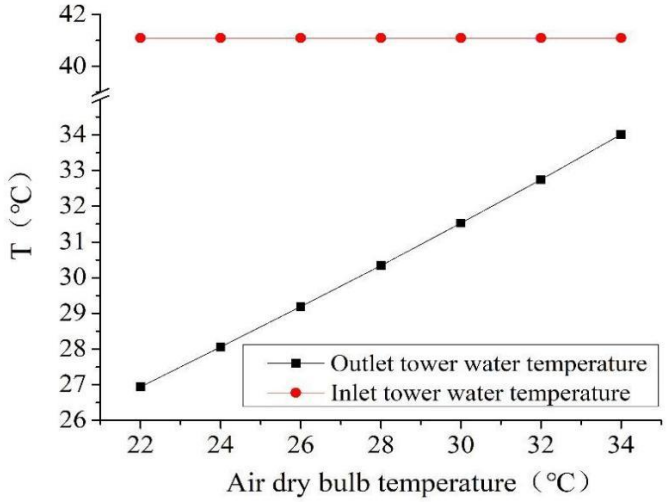

Figure 12. Outlet water temperature with different air-dry bulb temperature.

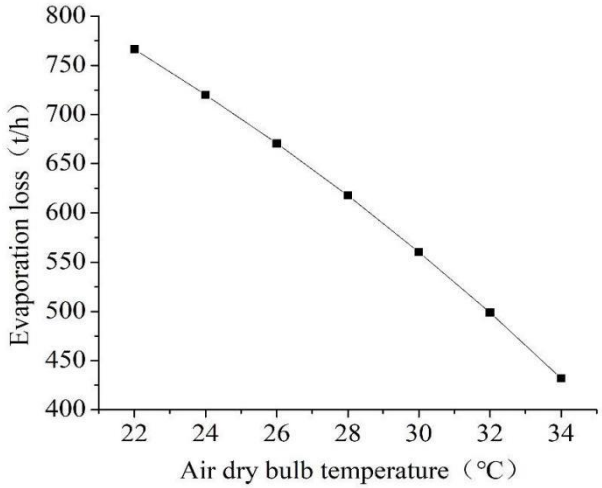

Figure 13. Evaporation loss at vary air dry bulb temperature.

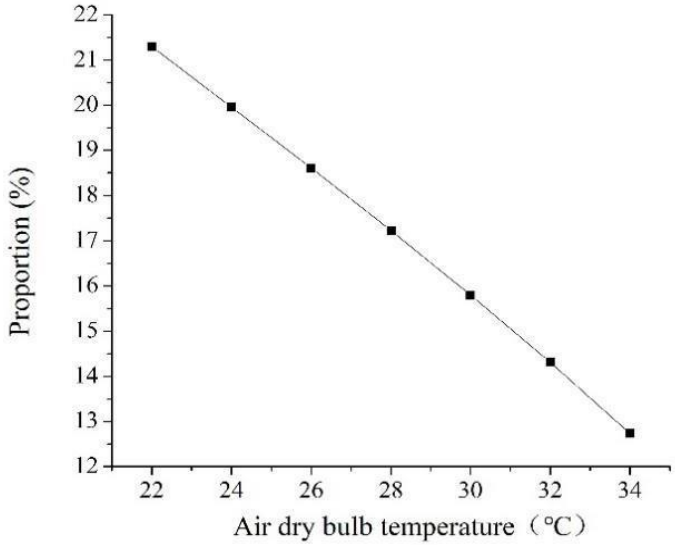

Figure 14. Relationship between the proportion of contact heat dissipation to total heat dissipation and air-dry bulb temperature.

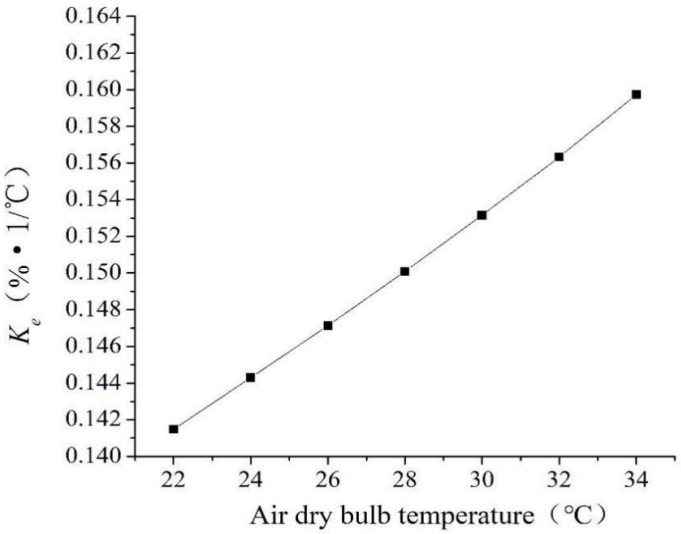

Figure 15. Relationship between K_e and air-dry bulb temperature.

5. Conclusions

In this study, the mathematical model for calculating the evaporation loss in the NDWCT was established. Taking NDWCTs in the representative 300 MW and 600 MW power plant as the research objects, the accuracy of the mathematical model was verified. The calculated results were quite in agreement with experimental values. The effect of air parameters on evaporation loss was emphatically studied.

With the air-dry bulb temperature increasing, the heat and mass transfer performance of the NDWCT deteriorates, the evaporation heat dissipation and the evaporation loss decreases. Reduction of the proportion of contact heat dissipation in total heat dissipation occurs, while the rate of evaporation loss caused by unit temperature difference increases. When air dry bulb temperature increased by 1 °C, the outlet tower water temperature increased by about 0.59 °C, and the evaporation loss dropped by nearly 26.65 t/h.

As the relative air humidity increases, the evaporation heat dissipation and the evaporation loss in NDWCT decreases. However, the ratio of the contact heat dissipation to the total heat dissipation increases, and the rate of evaporation loss caused by unit temperature difference decreases. When relative air humidity increased by 1%, the outlet water temperature rose by about 0.08 °C, and the evaporation loss decreased by about 5.63 t/h.

Author Contributions: Conceptualization, W.Y. and F.S.; data curation, F.S.; investigation, W.Y.; methodology, W.Y. and R.L.; validation, F.S., R.L., and X.C.; writing—original draft, W.Y.; writing—review & editing, Y.L. All authors have read and agreed to the published version of the manuscript.

Funding: This research received no external funding.

Conflicts of Interest: The authors declare no conflict of interest.

Nomenclature

A_t	fill surface area of the NDWCT (m^2)
A_v	surface area per unit volume of fill (m^2/m^3)
A_s	the area of cross section of fill (m^2)
c_p	specific heat at constant pressure (J/kg°C)
C, n	constants
g	gravitational acceleration (m/s^2)
h_d	mass-transfer coefficient (kg/m^2s)
H_{inlet}	tower inlet height (m)
H_t	the tower height (m)

H	pumping force of NDWCT (Pa)
i_{masw}	the enthalpy of the saturated air layer on the water surface when water temperature is T_w (J/kg)
i_{ma}	the enthalpy of the moist air when air temperature is T_a (J/kg)
j	the coordinates of the laps where the measuring point is located
K_e	the ratio of evaporation loss to total circulating water at per 1 °C temperature drop (%·1/°C)
k	heat coefficient
m	mass flow rate (kg/s)
m_{evap}	evaporation loss (t/h)
m_a	mass flow rate of air (kg/s)
m_w	mass flow rate of circulating water (kg/s)
Me	Merkel number
NDWCT	natural draft counter-flow wet cooling tower
Q_c	conduction heat dissipation in NDWCT (W)
Q_e	evaporation heat dissipation in NDWCT (W)
r_j	the radius of the measuring point in the lap j (m)
R	the radius of collecting basin (m)
T_w	water temperature (°C)
T_{w1}	inlet water temperature of the finite volume(°C)
T_{w2}	outlet water temperature of the finite volume(°C)
T_{wi}	inlet water temperature of NDWCT(°C)
T_{wo}	outlet water temperature of NDWCT (°C)
T_a	air temperature (°C)
T_{ai}	inlet air temperature of NDWCT(°C)
T_{ao}	outlet air temperature of NDWCT(°C)
v_{am}	the average airflow velocity in packing section (m/s)
z	height of the finite volume
Z	resistance of the NDWCT (Pa)

Greek Letters

ξ	total drag coefficient of tower
ρ_{ai}	tower inlet air density (kg/m^3)
ρ_{ao}	tower outlet air density (kg/m^3)
w	humidity ratio of air (kg/kg)
ε	the ratio of evaporation heat dissipation to total heat disspation
λ	air-water ratio
γ_{Tw2}	the latent heat of vaporization at the temperature of T_{w2} (kJ/kg)

Subscripts

a	air
c	conduction
e	evaporation
i	inlet
M	modification
m	mean, or mass transfer
o	outlet
s	saturation
t	tower
w	water

References

1. Feeley, T.J., III; Skone, T.J.; Stiegel, G.J.; McNemar, A.; Nemeth, M.; Schimmoller, B.; Murphy, J.T.; Manfredo, L. Water: A critical resource in the thermoelectric power industry. *Energy* **2008**, *33*, 1–11. [CrossRef]

2. Cutillas, C.G.; Ramírez, J.R.; Lucas, M. Optimum Design and Operation of an HVAC Cooling Tower for Energy and Water Conservation. *Energies* **2017**, *10*, 299. [CrossRef]
3. Macknick, J.; Newmark, R.L.; Heath, G.; Hallett, K.C. Operational water consumption and withdrawal factors for electricity generating technologies: A review of existing literature. *Environ. Res. Lett.* **2012**, *7*, 045802. [CrossRef]
4. Owen, M.T.F.; Kröger, D.G. An Investigation of Air-Cooled Steam Condenser Performance Under Windy Conditions Using Computational Fluid Dynamics. *J. Eng. Gas Turbines Power* **2011**, *133*, 064502. [CrossRef]
5. Yang, L.J.; Du, X.Z.; Yang, Y.P. Influences of wind-break wall configurations upon flow and heat transfer characteristics of air-cooled condensers in a power plant. *Int. J. Therm. Sci.* **2011**, *50*, 2050–2061. [CrossRef]
6. Zhang, L.; Zhang, L.; Zhang, Q.; Jiang, K.; Tie, Y.; Wang, S. Effects of the Second-Stage of Rotor with Single Abnormal Blade Angle on Rotating Stall of a Two-Stage Variable Pitch Axial Fan. *Energies* **2018**, *11*, 3293. [CrossRef]
7. Zhang, L.; He, R.; Wang, X.; Zhang, Q.; Wang, S. Study on static and dynamic characteristics of an axial fan with abnormal blade under rotating stall conditions. *Energy* **2019**, *170*, 305–325. [CrossRef]
8. Meyer, C.J.; Kroger, D.G. Numerical investigation of the effect of fan performance on forced draught air-cooled heat exchanger plenum chamber aerodynamic behaviour. *Appl. Therm. Eng.* **2004**, *24*, 359–371. [CrossRef]
9. Kairouani, L.; Hassairi, M.; Tarek, Z. Performance of cooling tower in south of Tunisia. *Build. Environ.* **2004**, *39*, 351–355. [CrossRef]
10. Xia, L.; Li, J.; Ma, W.; Gurgenci, H.; Guan, Z.; Wang, P. Water Consumption Comparison Between a Natural Draft Wet Cooling Tower and a Natural Draft Hybrid Cooling Tower—An Annual Simulation for Luoyang Conditions. *Heat Transf. Eng.* **2017**, *38*, 1034–1043. [CrossRef]
11. Facao, J.; Oliveira, A.C. Heat and Mass Transfer in an Indirect Contact Cooling Tower: CFD Simulation and Experiment. *Numer. Heat Transf. Part A Appl.* **2008**, *54*, 933–944. [CrossRef]
12. Qureshi, B.A.; Zubair, S.M. Prediction of Evaporation Losses in Wet Cooling Towers. *Heat Transf. Eng.* **2006**, *27*, 86–92. [CrossRef]
13. Qureshi, B.A.; Zubair, S.M. Prediction of evaporation losses in evaporative fluid coolers. *Appl. Therm. Eng.* **2007**, *27*, 520–527. [CrossRef]
14. Hajidavalloo, E.; Shakeri, R.; Mehrabian, M.A. Thermal performance of cross flow cooling towers in variable wet bulb temperature. *Energy Convers. Manag.* **2010**, *51*, 1298–1303. [CrossRef]
15. Rubio-Castro, E.; Serna-González, M.; Ponce-Ortega, J.M.; Morales-Cabrera, M.A. Optimization of mechanical draft counter flow wet-cooling towers using a rigorous model. *Appl. Therm. Eng.* **2011**, *31*, 3615–3628. [CrossRef]
16. Rao, R.V.; More, K.C. Optimal design and analysis of mechanical draft cooling tower using improved Jaya algorithm. *Int. J. Refrig.* **2017**, *82*, 312–324. [CrossRef]
17. Naik, B.K.; Muthukumar, P. A novel approach for performance assessment of mechanical draft wet cooling towers. *Appl. Therm. Eng.* **2017**, *121*, 14–26. [CrossRef]
18. Mansour, M.K.; Hassab, M.A. Innovative correlation for calculating thermal performance of counterflow wet-cooling tower. *Energy* **2014**, *74*, 855–862. [CrossRef]
19. Picardo, J.R.; Variyar, J.E. The Merkel equation revisited: A novel method to compute the packed height of a cooling tower. *Energy Convers. Manag.* **2012**, *57*, 167–172. [CrossRef]
20. Fisenko, S.P.; Brin, A.A.; Petruchik, A.I. Evaporative cooling of water in a mechanical draft cooling tower. *Int. J. Heat Mass Transf.* **2004**, *47*, 165–177. [CrossRef]
21. Chen, C.J.; Wang, R.Z.; Xia, Z.Z.; Kiplagat, J.K. Study on a silica gel–water adsorption chiller integrated with a closed wet cooling tower. *Int. J. Therm. Sci.* **2010**, *49*, 611–620. [CrossRef]
22. Gao, M.; Zou, J.; He, S.; Sun, F. Thermal performance analysis for high level water collecting wet cooling tower under crosswind conditions. *Appl. Therm. Eng.* **2018**, *136*, 568–575. [CrossRef]
23. Zhao, Z. *Cooling Tower*; Chinese Water Conservancy and Electric Power Publisher: Beijing, China, 2001.